Reactive and Functional Polymers 158 (2021) 104798

Contents lists available at ScienceDirect

Reactive and Functional Polymers

journal homepage: www.elsevier.com/locate/react

Perspective Article

Polyester-based photocrosslinkable bioadhesives for wound closure and tissue regeneration support

M. Santos [a,1], T. Cernadas [a,1], P. Martins [a], S.P. Miguel [b,c], I.J. Correia [a,b], P. Alves [a], P. Ferreira [a,*]

[a] CIEPQPF, Department of Chemical Engineering, University of Coimbra, P-3030 790 Coimbra, Portugal
[b] CICS-UBI, Health Sciences Research Center, University of Beira Interior, P-6200 506 Covilhã, Portugal
[c] CPIRN-IPG- Center of Potential and Innovation of Natural Resources, Polytechnic Institute of Guarda, Av. Dr. Francisco de Sá Carneiro, 6300-559 Guarda, Portugal

ARTICLE INFO

Keywords:
Oligomers
Functionalization
Photocrosslinking
Biocompatibility
Antimicrobial properties

ABSTRACT

Photocrosslinkable surgical adhesives provide many advantages when compared with traditional methods used in wound closure. This work aimed to develop UV-curable biodegradable adhesives based on lactic acid and PCL oligomers. Both materials were functionalized with 2-isocyanatoethyl acrylate (AOI). Subsequently, the photoinitiator (Irgacure® 2959) was added to the blend and then, the final materials were irradiated under UV light for two different times: 30 s and 2 min. After production of adhesives, its physicochemical properties were evaluated through FTIR-ATR and TGA, as well as its rheology, dynamic water contact angle, swelling capacity and hydrolytic degradation. Furthermore, the biocompatibility of the produced adhesives was also characterized in contact with human dermal fibroblasts cells. The antimicrobial activity of the materials was assessed by using *Staphylococcus aureus* and *Escherichia coli,* as bacterial models.

1. Introduction

In the past years, the growing interest in producing tissue adhesives and sealants that are able to improve the methods used to control blood loss and tissue healing in clinical applications [1,2], led to a rise in adhesive research and development [3–7]. It was estimated that, in 2017, adhesives, hemostats and sealants constituted a market share of approximately $38 billion [5].

The traditional surgical closure techniques are based on invasive procedures as sutures, staples, grafts and clips [4,5,8]. Despite their wide use, these methods have drawbacks associated to the risk of infection, (that retard the wound healing process), tissue damage, difficult handling, patient discomfort and poor cosmetic outcome [5,9,10]. In this way, the surgical adhesives have aroused interest as they promote bleeding control and wound closure in a simple, fast, non-invasive and effective way [4,10]. Adhesives are easy to apply, able to spread and adapt to the injured area and do not induce any tissue damage at the application site [5]. Spotnitz and Burks described the ideal adhesive as having the following characteristics: safety, efficacy, usability, low cost and FDA approvability [11]. The material and its metabolites should be biocompatible, do not induce any damage to the patient, must be effective when used for the designed application, easy to handle and apply and able to obtain certification from Food and Drug Administration (FDA) [10,11]. The use of this type of materials shortens the duration of surgery and patient hospitalization as well as reduce the return appointments, therefore, decreasing the cost of the overall procedure [11,12].

Bioadhesives can be classified as activated or instant, according to the crosslinking method [13]. The crosslinking of instant adhesives occurs by mixing two reactive components on a wet environment, which limits the handling and application time [14]. Also, this type of materials display specific mechanical properties that cannot be tailored to the application [13,14]. Activated adhesives include materials cured by UV, infrared or radiofrequency radiation, heat, and atmospheric plasma, allowing to control the duration and place of the 3D network formation and also monitoring the mechanical properties of the material, through the crosslinking extension [13–17]. The on-set polymerization of surgical adhesives is not yet widely used in clinical context, since almost all commercial products are instant type [13].

This work is focused on the development of UV photocrosslinkable adhesives prepared with two functionalized materials based on lactic acid oligomers and polycaprolactone (PCL). These polyesters are already approved by US Food and Drug Administration and widely used in the biomedical field, due to their degradability and biocompatibility

* Corresponding author.
E-mail address: pferreira@eq.uc.pt (P. Ferreira).
[1] These authors have made an equal contribution to the study.

https://doi.org/10.1016/j.reactfunctpolym.2020.104798
Received 9 September 2020; Received in revised form 7 December 2020; Accepted 9 December 2020
Available online 16 December 2020

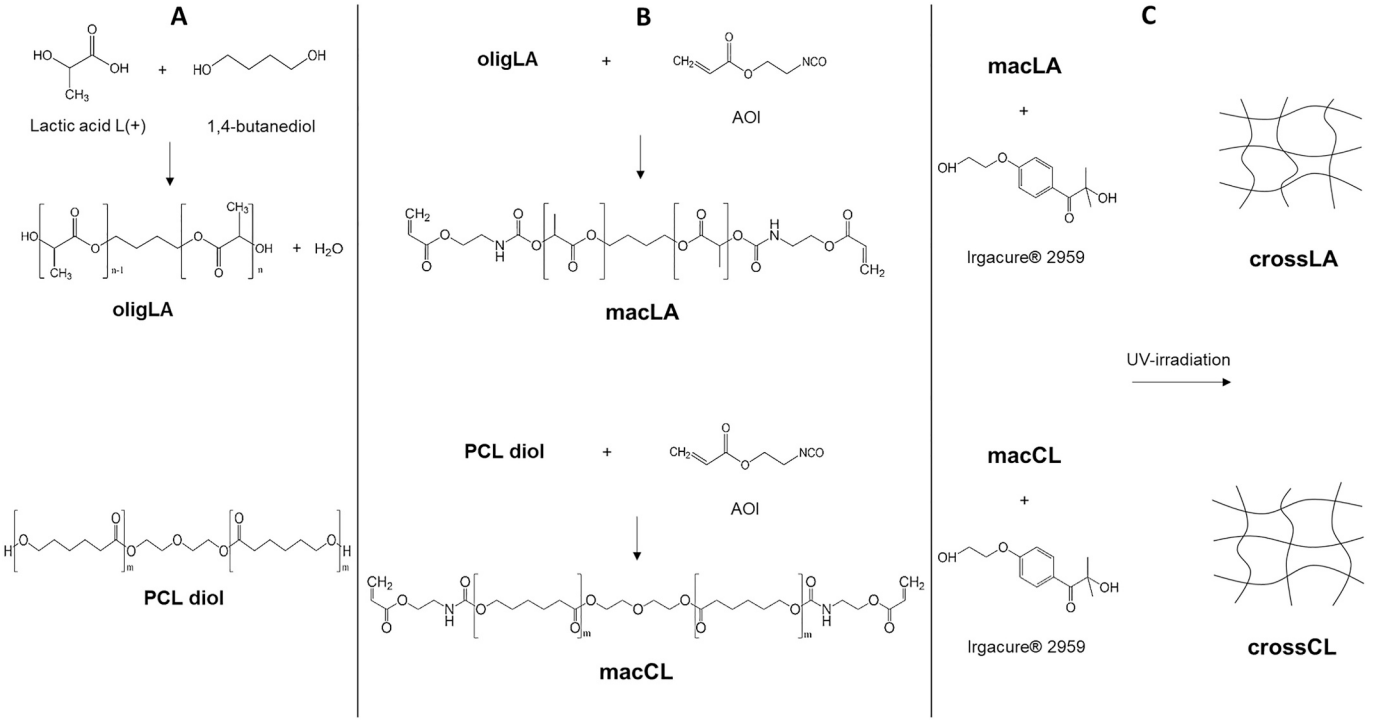

Fig. 1. Schematic representation of the materials synthesis. (A) Base materials: oligLA and PCL diol; (B) Macromers: macLA and macCL; (C) Crosslinked adhesives: crossLA and crossCL.

[18,19]. Lactic acid polymers are usually used in biodegradable sutures, clamps and scaffolds as they possess high degradation rates and lower mechanical integrity; PCL has a slower degradation rate and better mechanical properties and is generally used for long-term applications such as implants [18,20]. Therefore, these two materials were selected in order prepare photocrosslinkable, biocompatible and biodegradable materials in order to evaluate their suitability as wound closure support materials. For the functionalization reactions, the 2-isocyanoethyl acrylate (AOI) was selected. This compound is chemically similar to an isocyanate monomer already used in biomedical applications, 2-isocyanoethyl methacrylate (IEMA) [7,17,21–23]. AOI is available at a significantly lower price than IEMA, thus a good option to reduce the final cost of adhesives, making them more attractive from a market point of view. Irgacure® 2959 (Ir2959) was the selected biocompatible photoinitiator. The synthesized materials were crosslinked using two different irradiation times (30 s and 2 min) and were fully characterized.

2. Experimental procedures

2.1. Materials

Lactic Acid L(+) (80%) and PCL diol (530 g.mol^{-1}) were purchased from Sigma-Aldrich (Sintra, Portugal). Diethyl ether (99%), calcium chloride anhydrous (96%) and 1,4-butanediol (99%) were obtained from ACROS organics. The photoinitiator 2-hydroxy-1-[4-(2-hydroxyethoxy)phenyl]-2-methyl-1-propanone (Irgacure® 2959) and 2-Isocyanatoethyl acrylate (AOI, >98%)) were acquired from Ciba Specialty Chemicals and Tokyo Chemical Industry, respectively.

Fetal bovine serum (FBS) (free from any antibiotic) was acquired from Biochrom AG (Berlin, Germany). Normal Human Dermal Fibroblasts (NHDF) cells were purchased from PromoCell (Labclinics, S.A., Barcelona, Spain). 3-(4,5-Dimethylthiazol-2-yl)-2,5-diphenyltetrazolium bromide (MTT) was bought from Alfa Aesar (Ward Hill, USA). Amphotericin B, Dulbecco's modified Eagle's medium (DMEMF12), Trypsin were attained from Sigma-Aldrich (Sintra, Portugal). *Staphylococcus aureus* clinical isolate (*S. aureus*) ATCC 25,923 and *Escherichia coli* DH5 α (*E. coli*) were used as model organisms to evaluate the antimicrobial properties of the adhesives.

2.2. Methods

2.2.1. Synthesis of lactic acid oligomer

Firstly, the oligomer synthesis was performed through a polycondensation reaction. An aqueous solution of L(+) lactic acid (LA) (80%) was introduced into a 250 mL three-neck glass flask. The comonomer 1,4-butanediol was also added, according to the molecular weights and reaction stoichiometry (6:1). To ensure an inert atmosphere, a continuous nitrogen steam was inserted in the flask and to remove the water formed in the reaction, a reduction adapter was also added. After 9 h with mechanical stirring in an oil bath at 150 °C, the acid lactic oligomer (oligLA) was properly stored for later use (Fig. 1A).

2.2.2. Functionalization of lactic acid oligomers and PCL diol

The functionalization of the previously synthesized lactic acid oligomer (section 2.2.1) and low molecular weight PCL diol was performed using AOI, with equimolar ratio of NCO:OH groups (Fig. 1B).

The modification reactions occurred in similar conditions: 24 h in a stirred 100 mL three-neck volumetric flask, at 60 °C. In two separate reactions, PCL and oligLA were added to the glass flask and mixed with 10 mL of the solvent diethyl ether. Due to the high volatility of diethyl ether, a condenser was couplet, in order to promote solvent reflux. A drying tower filled with calcium chloride was also placed on top of the condenser, in order to prevent humidity from entering the reaction system. AOI was added carefully and quickly, in order to prevent contact with water, with which AOI strongly reacts. After 24 h of each reaction, liquid transparent functionalized macromers of oligLA-AOI (macLA) and PCL-AOI (macCL) were obtained.

2.2.3. Preparation of photocrosslinkable mixtures and UV irradiation

After raw materials synthesis and functionalization, the photoinitiator Ir2959® was added in a percentage of 4% of the carbon double bonds moles. During solubilization of Ir2959®, the mixture was kept in a

dark environment at the same operatory conditions of polymers functionalization (2.2.2). The base materials, macLA and macCL, were placed in glass plates and irradiated using a UV lamp (UVGL-58, Multiband UV-254/366 nm from *MineralLight*®) for 30 s and 2 min. After photocrosslinking, transparent and flexible films were obtained, crossLA and crossCL (Fig. 1C). To evaluate the crosslinking degree of the prepared materials, gel content assays were carried out by solvent extraction. Samples of each dried film were weighted (W_0) and placed in diethyl ether at room temperature and under stirring for 24 h. After being removed and dried under vacuum, the samples were weighted (W_1) and gel content percentage was calculated using Eq. (1).

$$\text{Gel Content } (\%) = \left(\frac{W_1}{W_0}\right) \times 100 \quad (1)$$

2.3. Characterization techniques

2.3.1. Attenuated Total reflectance - Fourier transform infrared spectroscopy (ATR-FTIR)

The obtained adhesives were characterized by ATR-FTIR analysis, using a Frontier FT-NIR/MIR spectrometer, from Perkin Elmer. Tests were performed at room temperature, with a resolution of 4 cm^{-1} and 64 scans.

2.3.2. Rheology

Rheological behaviour of macLA and macCL materials was assessed using a controlled stress rheometer (Haake RS1) using a plate/plate PP20-Ti geometry. The measurements were performed at 25 °C with a 0.2 mm GAP and a Phoenix thermocontroller. The resultant viscosities were evaluated as function of shear rate over time.

2.3.3. Water sorption capacity

In order to determine the swelling capacity, three samples of each adhesive were dried under vacuum conditions until constant weight (W_d) and then placed in a desiccator with a saturated solution of pentahydrated copper sulphate. All the samples were weighted at predetermined times until a maximum weight was achieved (W_s) and water sorption (%) was calculated by using Eq. (2).

$$\text{Water sorption } (\%) = \left(\frac{W_s - W_d}{W_d}\right) \times 100 \quad (2)$$

2.3.4. Hydrolytic degradation in phosphate buffer solution (PBS)

After drying the adhesives, three samples of each material were weighted ($W_{d,0}$), immersed in 5 mL of PBS 0.01 M (pH = 7.4), and then incubated at 37 °C for five weeks. At different stablished times, the films were removed from PBS, washed with distilled water and dried under vacuum, until constant weight ($W_{d,t}$). The degradation degree at each time was evaluated determining the weight loss as in Eq. (3)

$$\text{Weight loss } (\%) = \frac{W_{d,0} - W_{d,t}}{W_{d,0}} \times 100 \quad (3)$$

where $W_{d,0}$ and $W_{d,t}$ are the average samples weights before the immersion in PBS and after the immersion at time *t*, respectively.

2.3.5. Determination of dynamic contact angle profile

The dynamic contact angles of the crosslinked samples were measured in a Dataphysics OCA-20 contact angle analyzer (DataPhysics Instruments, Filderstadt, Germany) using the sessile drop method. A droplet of deionized water (10 μL) was automatically dispersed onto the sample surface and its evolution along time (120 s) was recorded with a CCD video camera attached to the equipment. The water contact angles were automatically calculated by the equipment software. The data obtained represents the mean values of three independent measurements.

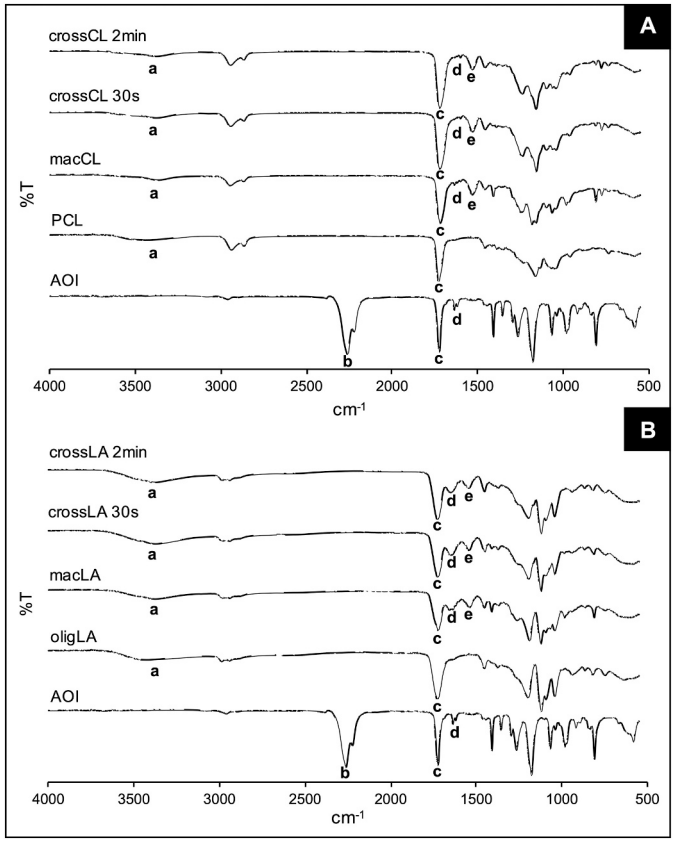

Fig. 2. FTIR-ATR spectra corresponding to (A) AOI, PCL, macCL and crossCL (30 s and 2 min irradiation); (B) AOI, oligLA, macLA and crossLA (30 s and 2 min irradiation).

2.3.6. Thermal properties

Thermal stabilities of AOI, LA and PCL diol as well as the ones of the synthesized materials before and after crosslinking were determined. Samples were subjected to thermo gravimetric analysis (TGA) in an SDT Q500 from Thermal Analysis (TA) Instruments. 5 to 10 mg of each material were heated to 600 °C with a heating rate of 10 °C/min, under nitrogen atmosphere at a flow rate of 100 mL/min.

2.3.7. Evaluation of films biocompatibility

NHDF cells were cultured in DMEM-F12, supplemented with 10% heat inactivated FBS, amphotericin B (100 g/ mL) and gentamicin (100 g/mL) in 75 cm^2 culture T-flasks. Cells were maintained in a humidified atmosphere at 37 °C, with 5% CO_2. In the first instance, the adhesives were placed into 96-well plates and sterilized by UV irradiation during 1 h. After that, to evaluate the cell adhesion and proliferation in the presence of the materials, the cells were seeded at a density of 10×10^3 cells per well. Cell growth was monitored using an Olympus CX41 inverted light microscope equipped with an Olympus SP-500 UZ digital camera.

In turn, the cytotoxic profile of the adhesives was evaluated through the MTT assay, which was performed according to the guidelines set by ISO 10993-5. In brief, the medium was replaced by 50 μL of MTT (5 mg/mL PBS) in each sample ($n = 5$), which were then incubated for 4 h, at 37 °C, in a 5% CO_2 atmosphere. Then, cells were treated with 200 μL of DMSO (0.04 N) for 30 min. A microplate reader (Biorad xMark microplate spectrophotometer) was used to read the absorbance at 570 nm of the samples from each well. Cells cultured without materials were used as negative control (K^-), whereas cells cultured with EtOH (96%) were used as positive control (K^+).

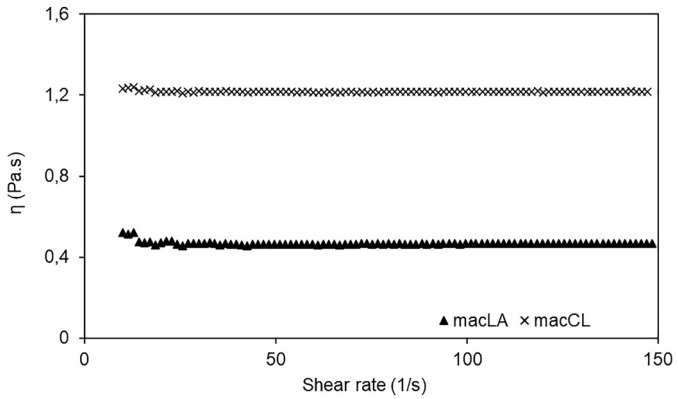

Fig. 3. Rheologic behaviour of the synthesized macromers.

2.3.8. Characterization of the antimicrobial properties of adhesives

To determine the antimicrobial properties of the films, *S. aureus* and *E.coli* were used as Gram-positive and Gram-negative bacteria model, respectively. To accomplish that, a modified Kirby-Bauer technique was used, where the bacteria at a concentration of 1×10^8 CFU/mL were dispensed onto an agar plate [24]. Then, circular adhesive films ($n = 3$) were placed on the agar plate and incubated during 24 h, at 37 °C. After that, the inhibitory halo diameter induced by the materials were photographed and measured using ImageJ (Scion Corp., Frederick, MD), image analysis software. Subsequently, SEM images were acquired to evaluate the bacterial colonization at the surface of the material, following the protocol reported in the literature [18,24].

2.3.9. Statistical analysis

The statistical analysis of the obtained results was performed using one-way analysis of variance (ANOVA), with the Newman-Keuls *post hoc* test. A p value lower than 0.05 ($p < 0.05$) was considered statistically significant.

3. Results and discussion

3.1. Chemical characterization

ATR-FTIR was performed to follow the adhesive synthesis and prove the success of the reactions. ATR-FTIR spectra of the final materials and its components are presented in Fig. 2 (A and B).

Analysing the AOI spectra, the typical band of elongation of isocyanate groups (N=C=O) is detected at 2262 cm^{-1} (b) [17,25]. In PCL spectra (Fig. 2A) can be observed the characteristic bands of hydroxyl (OH) and ester (C=O) groups at 3443 cm^{-1} (a) and 1731 cm^{-1} (c), respectively [17,19,25]. The FTIR results of macCL show the disappearance of the bands corresponding to PCL hydroxyl and AOI isocyanate groups, and the presence of C—N and N—H bands from urethane groups at 1531 cm^{-1} (e), suggesting that the functionalization occurred [17,26]. The carbon double bonds, essential to the materials photoreticulation, are present at 1600–1680 cm^{-1} (d) [19,26]. In the spectra corresponding to the irradiated adhesives (crossCL 30s and crossCL 2 min) C═C band is no longer detected, proving that the materials were successfully crosslinked.

Concerning the oligLA spectrum (Fig. 2B), it was also detected the characteristic bands from hydroxyl and ester groups (a and c). Comparing the AOI and oligLA spectra with the one from macLA, it can be observed that the isocyanate band is no longer present. In the macLA spectrum, the presence of characteristic urethane bands (e) is also detected. Analysing the crosslinked materials (crossLA 30s and crossLA 2 min), unlike what occurred in crossCL adhesives, there was no complete disappearance of the C═C bond (d), suggesting that the crossLA adhesives where not completely cured.

Table 1
UV irradiation times and corresponding gel content for the different prepared materials.

Adhesive	Curing time	Gel content (%)
crossLA	30 s	55.2 ± 0.92
	2 min	70.9 ± 1.18
crossCL	30 s	96.7 ± 0.40
	2 min	97.4 ± 0.63

3.2. Rheology

The rheological studies performed with the two synthesized macromers are represented in Fig. 3, with the viscosity (Pa.s) as function of shear rate (1/s).

The materials present Newtonian behaviour, since their viscosity remains constant with the increase of shear rate. The viscosity of this type of fluids is not influenced by the shear rate, depending only on the temperature. Both macromers present low viscosity, although the values obtained for macLA are lower than those for macCL (about 0.5 and 1.2 Pa.s, respectively). According to studies presented in the literature (including tests on commercial adhesives), the viscosity values obtained are within the desired range for this type of application, considering that the materials must be easy to apply, spread and adapt to the injured area, without compromising the strength of the material and without leading to unwanted migration and adhesion to the surrounding tissues [27–29].

3.3. Gel content

In order to evaluate the crosslinking performance of the prepared films, the gel content was determined, and the results are shown in Table 1.

The results presented in Table 1 showed that an increase on the UV irradiation time results in an increase of the gel content, and therefore the films become stiffer and more compact. This was clearly observed in crossLA films, where an increase of the exposure time, from 30 s to 2 min, improved the results from 55% to 71%, respectively.

Still, the degree of crosslinking of crossLA was lower than that of crossCL. This can be explained by comparing these results with those obtained by ATR-FTIR, which indicate that unlike crossCL adhesives, there was no complete disappearance of the C═C bond band, suggesting that crossLA adhesives would not be as effectively cured.

Furthermore, it was found that the film with the highest percentage

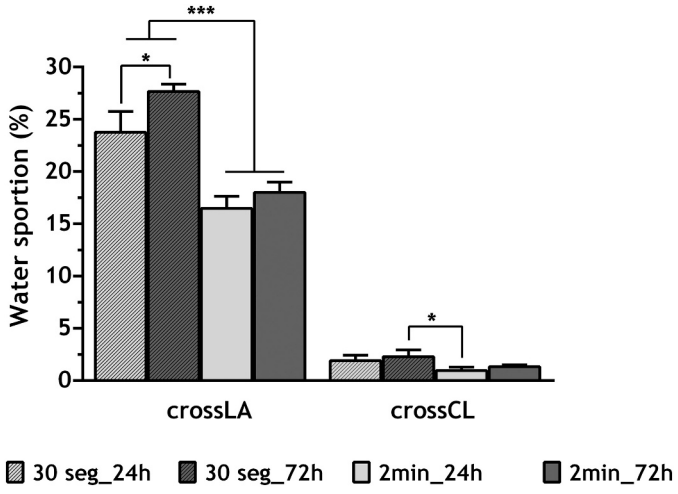

Fig. 4. Water sorption capacity of the produced adhesives, after 24 h and 72 h incubation. Data are presented as mean ± standard deviation, $n = 3$, $^*p < 0.05$, $^{***}p < 0.001$.

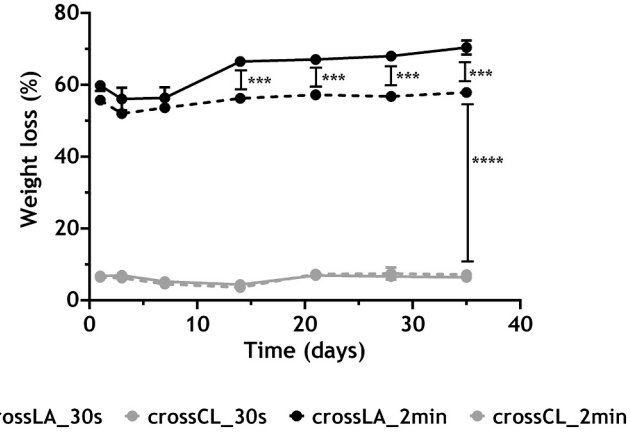

Fig. 5. Adhesives weight loss percentage (in PBS) over time. Data are presented as mean ± standard deviation, $n = 3$, ***$p < 0.001$, ****$p < 0.0001$.

of gel content was crossCL, with values of 97% for both times studied. Such result indicates that the 30s of exposure and the percentage of photoinitiator were adequate and sufficient to obtain a high level of C=C conversion and, therefore, allow the matrix to cure. Again, this is in line with the results obtained by ATF-FTIR.

3.4. Water sorption capacity

The swelling capacity of surgical adhesives is a very critical feature that determines the success of the treatment procedure. These adhesives are designed to help in the reconstitution of damaged tissues, so, their moderated volume increase will contribute to the hemostatic process without compromising the surrounding tissues [19,25]. An excessive swelling degree may lead to high compression of vascular structures, and/or cause inflammatory responses and inefficient cicatrisation [19,26].

Water sorption capacity of three samples of each synthesized material was monitored through 5 weeks in a closed container with pentahydrated copper sulphate saturated solution. After 72 h, the swelling capacity reached the maximum value. Fig. 4 shows the water sorption percentage of crossLA and crossCL (irradiated for 30 s and 2 min) after 24 and 72 h.

According to Fig. 4, the water sorption percentage decreases with the increase of irradiation time. Adhesives submitted to 2 min of UV radiation present lower swelling degrees than those that were crosslinked for only 30 s. Samples with 2 min irradiation time have a higher crosslinking degree (as shown by the gel content results), which makes the three-dimensional networks more stable, compact and insoluble, reducing the free space inside the polymeric matrix. Comparing the two materials, PCL based adhesives presented much lower water sorption capacity after 72 h (2.30 ± 0.64% and 1.33 ± 0.18%, compared to 27.67 ± 0.69% and 18.01 ± 0.98% for 30 s and 2 min irradiation, respectively), due to the hydrophobic character of this polymer.

All the results proved that the adhesives can be used for the intended purpose, since the obtained moderated swelling degrees fit the requisites necessary to this type of material.

3.5. Hydrolytic degradation in phosphate buffer solution (PBS)

Depending on the final use, bioadhesives should detach from de application site or be degraded and absorbed by the body [19,30]. In internal applications, the adhesive biodegradability is a very important factor [25]. To evaluate the films degradation profile, they were submitted to an environment similar to physiological conditions. Three samples of each photocrosslinked adhesive were placed in PBS at 37 °C and incubated for 5 weeks.

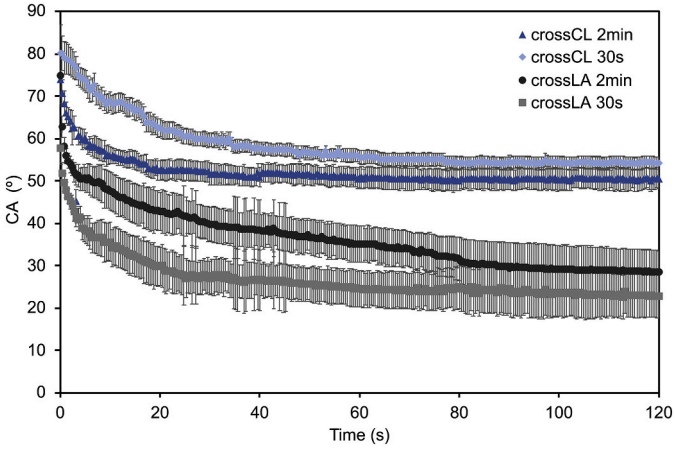

Fig. 6. Dynamic water contact angles for oligLA and macCL based crosslinked materials obtained with 30 s and 2 min UV irradiation.

According to Fig. 5, it can be verified that the higher weight loss percentage was registered for crossLA 30s, with 59.85 ± 1.49% in just 24 h and 70.42 ± 1.93% after 5 weeks. The higher water sorption capacity observed in crossLA adhesives, in addition to the ester bonds susceptibility to hydrolytic degradation, make these materials more biodegradable [7]. As for the crosslinking degree, longer irradiation times give rise to more compact adhesives, with less swelling capacity and, consequently, lower hydrolytic degradation.

CrossCL adhesives presented lower degradation values and, in this case, the irradiation time does not significantly influence the results. Due to the high stability of PCL and its hydrophobic character, the mass loss percentage was almost constant during the experiment time.

The adhesives behaviour is in agreement with the reported results concerning the gel content and swelling capacity of the materials. Since one of the most important properties for this type of application is the biodegradability of the materials, crossLA adhesives show more favorable degradation results than crossCL.

3.6. Determination of surface energy by contact angle measurement

The water contact angles (WCA) of the obtained adhesives were measured along time and the results are presented in Fig. 6.

Despite an initial similar WCA value from 70 to 80° for both crossCL and crossLA, the different adhesives showed a similar profile but different final WCA values. As expected, PCL-based adhesives present higher WCA when compared with the PLA-based ones, due to the strong hydrophobic character of PCL [31,32]. These results denote that crossLA adhesives showed higher wettability than crossCL, with a final WCA of around 30° against 55°. Moreover, for both crossLA and crossCL, the WCA trace obtained are very similar for the different crosslinking times (2 min and 30 s), which lead to the conclusion that the irradiation time does not influence the wettability of the adhesives.

The obtained results are in line with the hydrolytic degradation results, which showed a low degradation for crossCL, due to its hydrophobicity. While crossLA, a more hydrophilic adhesive, presented high hydrolytic degradation.

3.7. Thermal properties

Thermal stabilities of initial materials AOI, PCL and LA, as well as macCL and macLA before and after photoirradiation (30 s and 2 min) were evaluated by TGA, under nitrogen atmosphere (Fig. 7A to Fig. 7F).

The results obtained through TGA analyses showed that AOI presents a single degradation mechanism that is visible as a sharp and narrow peak in the derivative curve of the thermogram with a maximum of 106.5 °C.

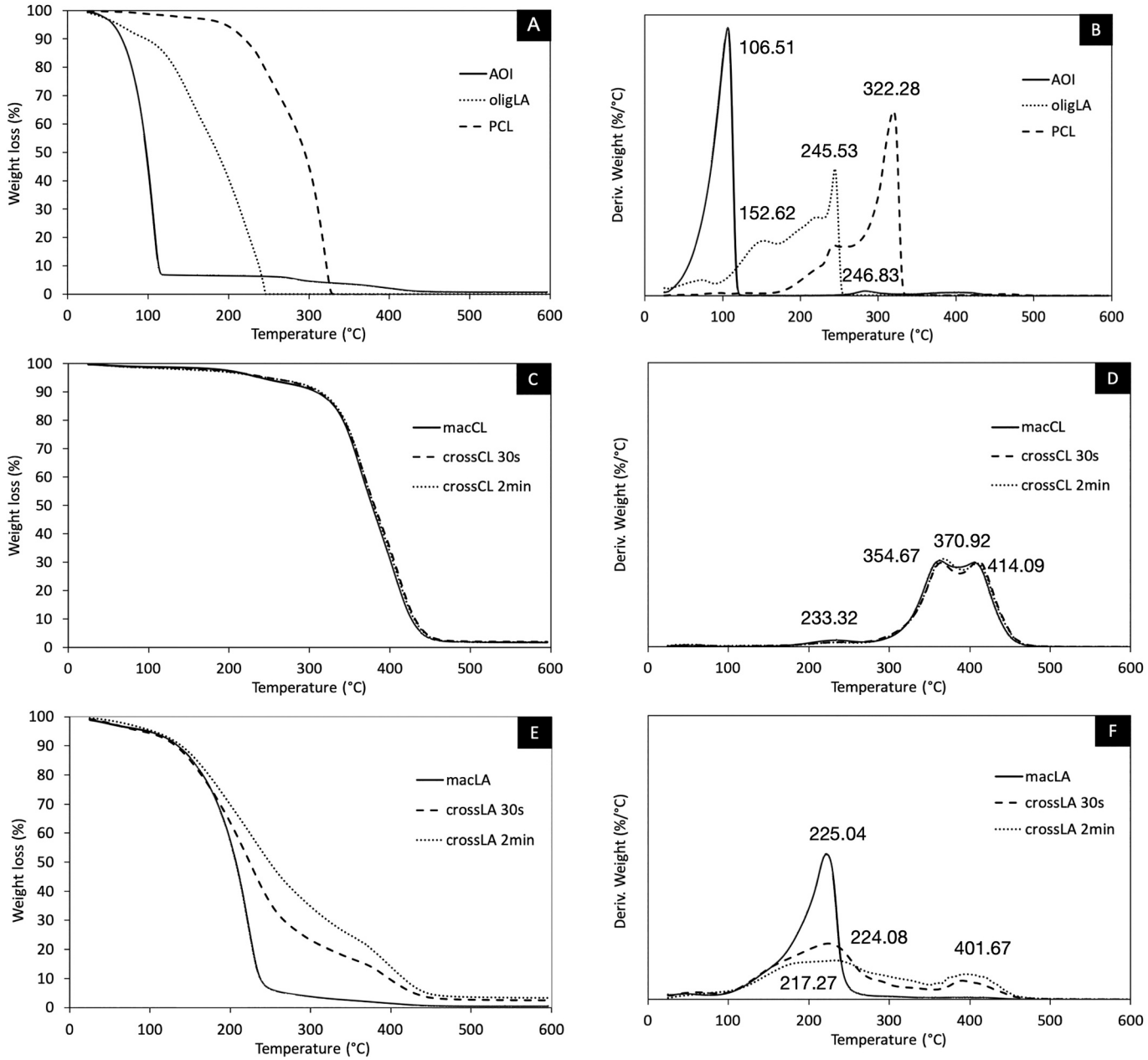

Fig. 7. (A) Thermogravimetric traces obtained for starting materials AOI, oligLA and PCL and (B) correspondent DTG thermograms. (C) Thermogravimetric traces obtained for oligLA macromer and crosslinked oligLA based materials and (D) correspondent DTG thermograms. (E) Thermogravimetric traces obtained for macCL macromer and crosslinked macCL based materials and (D) correspondent DTG thermograms. Thermal characterization was performed at a heating rate of 10 °C/min.

Considering PCL, it was verified that thermal degradation of PCL occurred in two stages at 246.8 and 322.3 °C suggesting a double degradation mechanism. These results have been previously reported by other authors [33] that concluded that the first degradation step is due to the break of polyester chains *via* ester pyrolysis reaction resulting in water, CO_2 and carboxylic acid formation. The second degradation step involves the depolymerization of the PCL chains resulting in the formation of cyclic ε-caprolactone.

The registered thermogram for the lactic acid oligomer displays a three-stage decomposition mechanism. The first one, occurring before 100 °C (weight loss of 9.8%), represents the volatilization of the remaining water in the oligomer's structure. Moreover, a small curve inflexion, with a maximum value of 152.64 °C may be seen, which may be ascribed to the volatilization of some unreacted lactic acid, as previously reported by other studies [34]. The increased value of this temperature during analysis can be explained by the entrapment of the lactic acid molecules in the viscous oligomer and therefore require a larger amount of energy to volatize. The third mass loss step that starts at 232.22 °C with the maximum T_d at 245.78 °C is attributed to the thermal degradation of the ester bonds of the oligomer and is coherent with previously obtained results [25].

Considering the PCL macromer, slight differences were observed between the macCL and both the crosslinked materials. All three samples present a thermal degradation profile that occurs in three stages. The first, a minor transition at around 223.32 °C corresponds to the degradation of the urethane bonds resulting in carbon dioxide and monoxide, amines and aldehydes [35]. The second step was registered at 354.67 °C for the macromer and around 370.92 °C for the crosslinked materials and is ascribed to the degradation of ester bonds in the soft segments of the urethanes. The value of this degradation temperature is

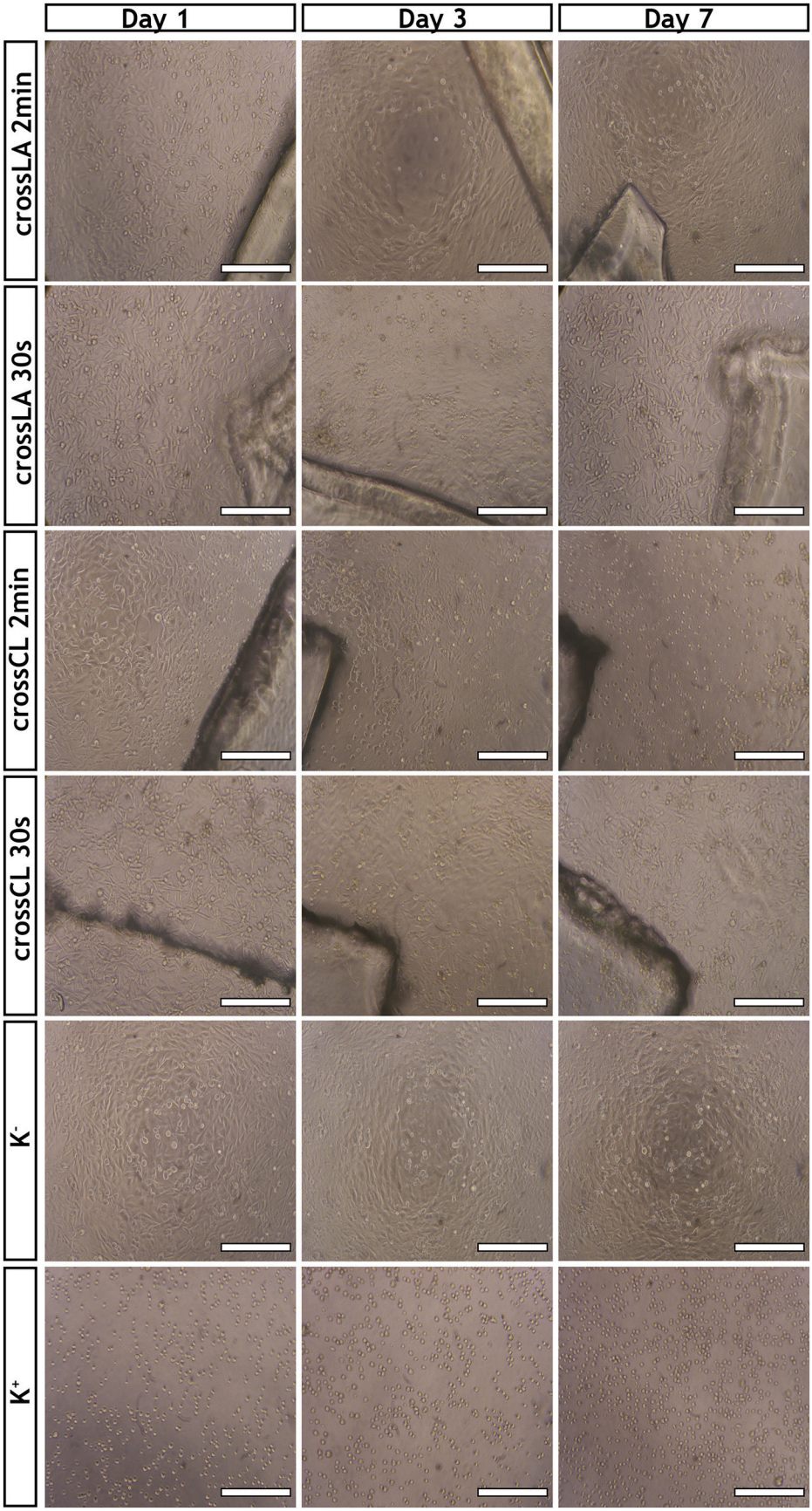

Fig. 8. Optical microscopic images of Normal Human Dermal Fibroblast (NHDF) cells cultured in the presence of produced adhesives (crossLA 30s, crossLA 2 min, crossCL 30s and crossCL 2 min) during 1, 3, and 7 days; K^- (negative control); K^+ (positive control). Scale bar represents 200 μm.

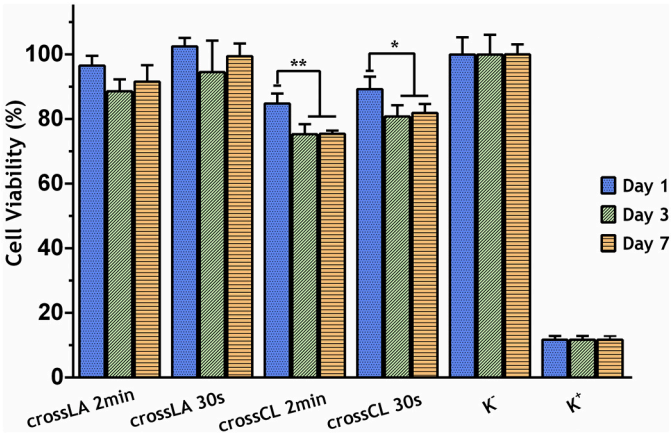

Fig. 9. Characterization of the adhesives' cytotoxic profile through the quantification of NHDF viability when they seeded in contact with materials during 1, 3 and 7 days. K^- (negative control); K^+ (positive control). Data are presented as the mean ± standard deviation, $n = 5$, $^*p < 0.05$; $^{**}p < 0.01$.

significantly higher for the functionalized PCL than for original one. This increase in thermal stability is justified by urethane hard segments in the polymeric backbone, which allow the establishment of hydrogen bonds between urethanes NH and CO/C=O groups [36]. Finally, the last degradation at 414.09 °C is attributed to the decomposition of higher energy bonds such as C=O, C=C, C—O and C—H bonds [35].

Analysing the lactic acid-based materials, it is possible to verify that results were distinct for the macromer and the crosslinked materials. The macLA thermogram shows a one stage degradation profile with a T_d at 225.04 °C attributed to the degradation of the ester bonds of the oligomer as well as the degradation of the urethane bonds. However, after UV crosslinking, thermal stability of the materials increases for higher temperature values. While a 96.11% of mass loss was registered for the macromer macLA at 300 °C, these same values of degradation were only registered at 441.20 °C and 472.85 °C for the crossLA 30 s and crossLA 2 min, respectively. Moreover, at 500 °C, all the materials were completely degraded.

3.8. Evaluation of adhesives' biocompatibility

The cytotoxic profile of the adhesive was evaluated by using NHDF as model cells, since these cells play crucial roles in the wound healing process, namely in the production of extracellular matrix [24,32].

After cell seeding in contact with adhesives, optical microscopic images were acquired after 1, 3 and 7 days of incubation, as presented in Fig. 8. The images show that the NHDF cells exhibit a similar morphology to those of K^- (cells incubated with culture medium), revealing that the adhesives did not induce any morphological alteration to the human fibroblast cells.

Furthermore, the cell viability was also quantified by performing an MTT assay during 1, 3 and 7 days. The number of viable cells present in each well is proportional to the amount of the purple formazan crystals produced in each well [32,37]. The results obtained from MTT assay (Fig. 9) show that the crossLA and crossCL adhesives at both UV-radiation times, did not affect the cell viability for 7 days. Nevertheless, the crossCL adhesives presented a decrease in cell viability after 3 and 7 days of incubation.

Taking into account these *in vitro* results, it is possible to verify that the crossLA adhesives exhibit a better biological performance to be used as bioadhesive for wound closure. Such results are in agreement with the high swelling capacity and low water contact angle displayed by crossLA adhesives. These features are fundamental to provide a suitable environment for cell proliferation and adhesion. In fact, the improved biological properties of the hydrophilic and lactic acid-based materials have been widely reported in the literature [38,39].

3.9. Evaluation of antimicrobial properties of films

The bacterial contamination of the wound site can lead to severe and devastating complications, that impair the progression of healing process [40]. Considering this, the production of surgical adhesives

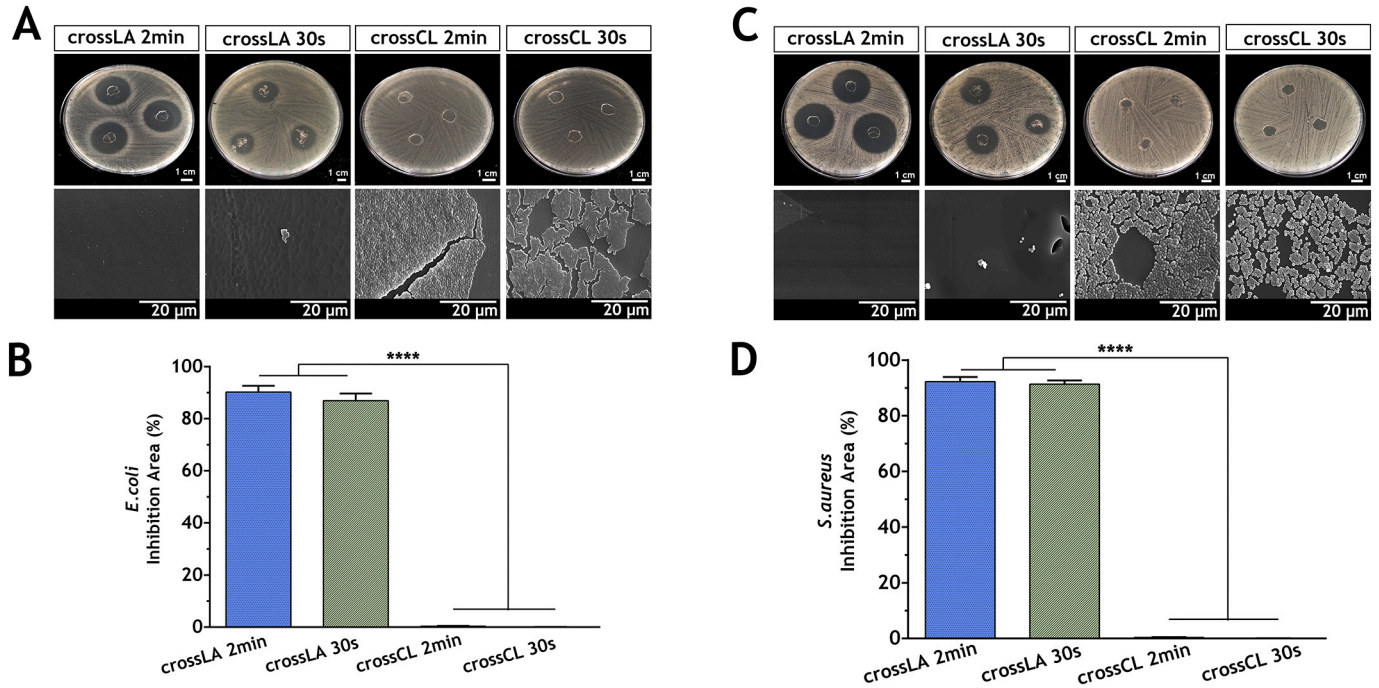

Fig. 10. Evaluation of the antimicrobial properties of the produced adhesives against *E. coli* and S.aureus: macroscopic images of the inhibition halos and SEM images of bacterial growth at adhesives' surface (A and C); determination of the inhibition area presented by the adhesives (B and D). Data are presented as the mean ± standard deviation, $n = 3$, $^{****}p < 0.0001$.

exhibiting antimicrobial activity is an attractive therapeutic strategy to avoid bacterial colonization and hence improve the wound healing process [18,38,41,42].

Herein, the antimicrobial properties of the adhesives were determined by using *E. coli* (gram-negative bacterium) and *S. aureus* (gram-positive bacterium) as bacterial models (Supplementary Fig. S1). The inhibitory area exhibited by the adhesives were determined and the bacterial colonization at materials' surface was characterized by SEM analysis (Fig. 10).

The results presented in Fig. 10A and B clearly evidenced that the crossLA adhesives displayed a high antimicrobial effect against *E.coli* growth, exhibiting an inhibition area of 90.2 ± 2.4%, 86.90 ± 2.8% for crossLA 2 min and crossLA 30s, respectively. Unlike, the crossCL adhesives were unable to avoid the *E.coli* growth, presenting the minimal inhibition area values of 0.23 ± 0.23% and 0.13 ± 0.06% for crossCL 2 min and crossCL 30s, respectively.

Similar results were also attained, when the adhesives were incubated with *S.aureus* (as shown in Fig. 10C and D), where higher inhibition area values were noticed for crossLA adhesives (92.3 ± 1.7% (2 min) and 91.4 ± 1.3% (30 s)) in comparison to those presented by crossCL adhesives (0.23 ± 0.23% (2 min) and 0.13 ± 0.06% (30 s)). Such differences on antimicrobial activity between crossLA and crossCL adhesives were also observed in SEM images, where it was possible to visualize the bacterial colonization of *E.coli* and *S.aureus* only at the surface of crossCL adhesives. Such results may be explained by the hydrophobic character of PCL and its non-antimicrobial activity [37,43].

On the other side, the antimicrobial activity exhibited by crossLA adhesives corroborate the weight loss results, where it was verified that these adhesives lost ≈ 60% of its total weight. Such rapid weight loss of the crossLA adhesives leads to the release of the lactic acid oligomers, which can disrupt the cytoplasmic membranes, the content and activity of bacterial proteins [44].

According to the data reported in the literature, the antibacterial action of the lactic acid is essentially attributed to its ability to penetrate the cytoplasmic membrane, resulting in reduced intracellular pH and disruption of the transmembrane proton motive force, resulting in the bacterial dead [45].

4. Conclusions

In this research work, which aimed to prepare materials for use as surgical adhesives, a L-lactic acid oligomer (previously synthesized) and PCL diol were functionalized with AOI, in order to introduce carbon double bonds in the polymer structure. The viscosity of these materials was evaluated and it was concluded that it fits the desired values for this type of applications. The biocompatible photoinitiator Irgacure® 2959 was added to the resulting macromeres, which were later crosslinked by UV irradiation for 30 s and 2 min. The chemical reactions of synthesis, functionalization and crosslinking were confirmed by the FTIR-ATR results.

The prepared materials were also characterized regarding their gel content, water sorption capacity and hydrolytic degradation. Due to the lower crosslinking degree of crossLA, the gel content results of this material were also inferior. CrossCL samples presented high gel content percentages, very similar for both irradiation times. Swelling and hydrolytic degradation results also demonstrated that the UV exposure time in crossCL adhesives has little influence on the final material behaviour, showing that, in this case, 30 s would be a suitable irradiation period. The hydrophobic character of PCL leads to reduced swelling degree and consequently, low susceptibility to hydrolytic degradation. CrossLA adhesives presented higher values of swelling and weight loss, decreasing with increasing irradiation time.

Coherent results were obtained for dynamic contact angles assays during which similar WCA values were obtained for both irradiation times indicating that this factor did not influence the wettability of these materials. Similarly, TGA analyses showed that the thermal stabilities of the crosslinked materials were also not influenced by UV irradiation time.

The *in vitro* assays demonstrated that the crossLA adhesives presented a better biological performance, since the human fibroblasts viability was not compromised during 7 days of incubation. Furthermore, the antimicrobial assays also evidenced the more pronounced antimicrobial effect of crossLA bioadhesives against growth of *E.coli* and *S.aureus*.

Based on all gathered data, the biodegradable photocrosslinkable adhesives, in particular crossLA exhibited the most promising properties to be used as adhesive for wound healing applications. In near future, *ex vivo/in vivo* assays may be performed to evaluate the ability of the crossLA films to adhere animal tissues.

Supplementary data to this article can be found online at https://doi.org/10.1016/j.reactfunctpolym.2020.104798.

Data availability

The raw/processed data required to reproduce these findings cannot be shared at this time due to technical or time limitations. However, correspondance author will provide the required materila if contacted.

Declaration of Competing Interest

The authors declare that they have no known competing financial interests or personal relationships that could have appeared to influence the work reported in this paper.

Acknowledgements

This work was supported by the Portuguese Foundation for Science and Technology through the project FCT Researcher (IF/01432/2015), project ZAPGO (PTDC/NAN-MAT/28989/2017) and project INEYE (PTDC/EMD-EMD/31462/2017). The authors from CIEPQPF were supported by Fundação para a Ciência e a Tecnologia (FCT) UID/EQU/00102/2019.

References

[1] J. Qu, X. Zhao, Y. Liang, T. Zhang, P.X. Ma, B. Guo, Antibacterial adhesive injectable hydrogels with rapid self-healing, extensibility and compressibility as wound dressing for joints skin wound healing, Biomaterials 183 (July) (2018), pp. 185–ill.
[2] Y. Liang, et al., Adhesive hemostatic conducting injectable composite hydrogels with sustained drug release and photothermal antibacterial activity to promote full-thickness skin regeneration during wound healing, Small 15 (12) (2019) 1–17.
[3] J.C. Wheat, J.S. Wolf, Advances in bioadhesives, tissue sealants, and hemostatic agents, Urol. Clin. North Am. 36 (2) (2009) 265–275.
[4] M. Mehdizadeh, J. Yang, Design strategies and applications of tissue bioadhesives, Macromol. Biosci. 13 (3) (2013) 271–288.
[5] V. Bhagat, M.L. Becker, Degradable adhesives for surgery and tissue engineering, Biomacromolecules 18 (10) (2017) 3009–3039.
[6] M.L.B. Palacio, B. Bhushan, Research article: bioadhesion: a review of concepts and applications, Philos. Trans. R. Soc. A Math. Phys. Eng. Sci. 370 (1967) (2012) 2321–2347.
[7] D.R.S. Travassos, et al., Engineering star-shaped lactic acid oligomers to develop novel functional adhesives, J. Mater. Res. 33 (10) (2018) 1463–1474.
[8] M. Kazemzadeh-Narbat, N. Annabi, A. Khademhosseini, Surgical sealants and high strength adhesives, Mater. Today 18 (4) (2015) 176–177.
[9] A.P. Duarte, J.F. Coelho, J.C. Bordado, M.T. Cidade, M.H. Gil, Surgical adhesives: systematic review of the main types and development forecast, Prog. Polym. Sci. 37 (8) (2012) 1031–1050.
[10] F. Scognamiglio, et al., Adhesive and sealant interfaces for general surgery applications, J. Biomed. Mater. Res. - Part B Appl. Biomater. 104 (3) (2016) 626–639.
[11] W.D. Spotnitz, S. Burks, Hemostats, sealants, and adhesives: components of the surgical toolbox, Transfusion 48 (7) (2008) 1502–1516.
[12] F.P. Robertson, L.J. Magill, C. Davidson, H. Mitchell, B.R. Davidson, Cyanoacrylate tissue glues for cutaneous wound closure, Wound Heal. Biomater. 2 (2016) 151–168.
[13] R.D. O'Rorke, et al., Addressing unmet clinical needs with UV bioadhesives, Biomacromolecules 18 (3) (2017) 674–682.
[14] E.M. Petrie, Cyanoacrylate adhesives in surgical applications, Prog. Adhes. Adhes. (2015) 245–298, no. August 2014.

[15] G. Feng, I. Djordjevic, V. Mogal, R. O'Rorke, O. Pokholenko, T.W.J. Steele, Elastic light tunable tissue adhesive dendrimers, Macromol. Biosci. (2016) 1072–1082.
[16] R.S. Benson, Use of radiation in biomaterials science, Nucl. Inst. Methods Phys. Res. B 191 (1–4) (2002) 752–757.
[17] D.S. Marques, et al., Functionalization and photocuring of an L-lactic acid macromer for biomedical applications, Int. J. Polym. Mater. Polym. Biomater. 65 (10) (2016) 497–507.
[18] T.M. Cernadas, et al., Preparation of biodegradable functionalized polyesters aimed to be used as surgical adhesives, Eur. Polym. J. 117 (2019) 442–454. May.
[19] T. Cernadas, et al., Functionalized polyester-based materials as UV curable adhesives, Eur. Polym. J. 120 (June) (2019) 109–196.
[20] B. Guo, P.X. Ma, Synthetic biodegradable functional polymers for tissue engineering: a brief review, Sci. China Chem. 57 (4) (2014) 490–500.
[21] A.S. Karikari, W.F. Edwards, J.B. Mecham, T.E. Long, Influence of peripheral hydrogen bonding on the mechanical properties of photo-cross-linked star-shaped poly(D,L-lactide) networks, Biomacromolecules 6 (5) (2005) 2866–2874.
[22] A.P. Vieira, P. Ferreira, J.F.J. Coelho, M.H. Gil, Photocrosslinkable starch-based polymers for ophthalmologic drug delivery, Int. J. Biol. Macromol. 43 (4) (2008) 325–332.
[23] J.F. Almeida, P. Ferreira, A. Lopes, M.H. Gil, Photocrosslinkable biodegradable responsive hydrogels as drug delivery systems, Int. J. Biol. Macromol. 49 (5) (2011) 948–954.
[24] S.P. Miguel, D. Simões, A.F. Moreira, R.S. Sequeira, I.J. Correia, Production and characterization of electrospun silk fibroin based asymmetric membranes for wound dressing applications, Int. J. Biol. Macromol. 121 (2019) 524–535.
[25] J.M.C. Santos, et al., Synthesis, functionalization and characterization of UV-curable lactic acid based oligomers to be used as surgical adhesives, React. Funct. Polym. J. 94 (2015) 43–54.
[26] P. Ferreira, J.F.J. Coelho, M.H. Gil, Development of a new photocrosslinkable biodegradable bioadhesive, Int. J. Pharm. 352 (1–2) (2008) 172–181.
[27] P.J. Sniezek, et al., A randomized controlled trial of high-viscosity 2-octyl cyanoacrylate tissue adhesive versus sutures in repairing facial wounds following Mohs micrographic surgery, Dermatol. Surg. 33 (8) (2007) 966–971.
[28] A.J. Singer, L. Perry, A comparative study of the surgically relevant mechanical characteristics of the topical skin adhesives, Acad. Emerg. Med. 19 (11) (2012) 1281–1286.
[29] T. Hayashi, M. Hasegawa, J. Inamasu, K. Adachi, S. Nagahisa, Y. Hirose, Experimental study on the viscosity and adhesive performance of exogenous liquid fibrin glue, Neurol. Med. Chir. (Tokyo) 54 (11) (2014) 895–900.
[30] P. Ferreira, M.H. Gil, P. Alves, An overview in surgical adhesives, in: A. McFarland, M. Akins (Eds.), Recent Advances in Adhesions Research, no. March 2016, Nova Science Publishers, Inc., N. Y., 2013, pp. 59–86.
[31] P. Ferreira, et al., Photocrosslinkable electrospun fiber meshes for tissue engineering applications, Eur. Polym. J. 97 (October) (2017) 210–219.
[32] P. Alves, et al., Photocrosslinkable nanofibrous asymmetric membrane designed for wound dressing, Polymers (Basel). 11 (4) (2019) 1–18.
[33] O. Persenaire, M. Alexandre, P. Degée, P. Dubois, Mechanisms and kinetics of thermal degradation of poly(ε-caprolactone), Biomacromolecules 2 (1) (2001) 288–294.
[34] A. Komesu, P.F. Martins Martinez, B.H. Lunelli, J. Oliveira, M.R. Wolf MacIel, R. MacIel Filho, Study of lactic acid thermal behavior using thermoanalytical techniques, J. Chemother. 2017 (2017).
[35] M. Malik, R. Kaur, Mechanical and thermal properties of castor oil–based polyurethane adhesive: effect of TiO2 filler, Adv. Polym. Technol. 37 (1) (2018) 21637.
[36] M.F. Valero, Y. Ortegón, Polyurethane elastomers-based modified castor oil and poly(ε-caprolactone) for surface-coating applications: synthesis, characterization, and in vitro degradation, J. Elastomers Plast. 47 (4) (2013) 360–369.
[37] D.R. Figueira, S.P. Miguel, K.D. de Sá, I.J. Correia, Production and characterization of polycaprolactone- hyaluronic acid/chitosan- zein electrospun bilayer nanofibrous membrane for tissue regeneration, Int. J. Biol. Macromol. 93 (2016) 1100–1110.
[38] D.S. Marques, et al., Photocurable bioadhesive based on lactic acid, Mater. Sci. Eng. C 58 (2016) 601–609.
[39] V.K. Arvind Guptaa, Neha Mulchandania, Manisha Shahb, Sachin Kumarb, Functionalized chitosan mediated stereocomplexation of poly(lactic acid): influence on crystallization, oxygen permeability, wettability and biocompatibility behavior, Polymer (Guildf). 142 (2018) 196–208.
[40] D. Simões, S.P. Miguel, M.P. Ribeiro, P. Coutinho, A.G. Mendonça, I.J. Correia, Recent advances on antimicrobial wound dressing: a review, Eur. J. Pharm. Biopharm. 127 (February) (2018) 130–141.
[41] L.W. Xinchen Du, Le Wu, Hongyu Yan, Qu Lijie, Lina Wang, Xin Wang, Shuo Ren, Deling Kong, Multifunctional hydrogel patch with toughness, tissue adhesiveness, and antibacterial activity for sutureless wound closure, ACS Biomater. Sci. Eng. 5 (5) (2019) 2610–2620.
[42] N. Han, et al., A Fe3+−crosslinked pyrogallol-tethered gelatin adhesive hydrogel with antibacterial activity for wound healing, Biomater. Sci. 8 (11) (2020) 3164–3172.
[43] S.P. Miguel, M.P. Ribeiro, P. Coutinho, I.J. Correia, Electrospun polycaprolactone/Aloe Vera_chitosan nanofibrous asymmetric membranes aimed for wound healing applications, Polymers (Basel). 9 (5) (2017).
[44] C. Wang, T. Chang, H. Yang, M. Cui, Antibacterial mechanism of lactic acid on physiological and morphological properties of Salmonella enteritidis, *Escherichia coli* and listeria monocytogenes, Food Control 47 (2015) 231–236.
[45] B. Ray, Food Biopreservatives of Microbial Origin, CRC press, 2019.